Published OnlineFirst December 10, 2014; DOI: 10.1158/1535-7163.MCT-14-0647

Small Molecule Therapeutics

Molecular Cancer Therapeutics

Evaluation of the *In Vitro* and *In Vivo* Efficacy of the JAK Inhibitor AZD1480 against JAK-Mutated Acute Lymphoblastic Leukemia

Santi Suryani[1], Lauryn S. Bracken[1], Richard C. Harvey[2], Keith C.S. Sia[1], Hernan Carol[1], I-Ming Chen[2], Kathryn Evans[1], Philipp A. Dietrich[1], Kathryn G. Roberts[3], Raushan T. Kurmasheva[4], Catherine A. Billups[5], Charles G. Mullighan[3], Cheryl L. Willman[2], Mignon L. Loh[6], Stephen P. Hunger[7], Peter J. Houghton[4], Malcolm A. Smith[8], and Richard B. Lock[1]

Abstract

Genome-wide studies have identified a high-risk subgroup of pediatric acute lymphoblastic leukemia (ALL) harboring mutations in the Janus kinases (JAK). The purpose of this study was to assess the preclinical efficacy of the JAK1/2 inhibitor AZD1480, both as a single agent and in combination with the MEK inhibitor selumetinib, against JAK-mutated patient-derived xenografts. Patient-derived xenografts were established in immunodeficient mice from bone marrow or peripheral blood biopsy specimens, and their gene expression profiles compared with the original patient biopsies by microarray analysis. JAK/STAT and MAPK signaling pathways, and the inhibitory effects of targeted drugs, were interrogated by immunoblotting of phosphoproteins. The antileukemic effects of AZD1480 and selumetinib, alone and in combination, were tested against JAK-mutated ALL xenografts both *in vitro* and *in vivo*. Xenografts accurately represented the primary disease as determined by gene expression profiling. Cellular phosphoprotein analysis demonstrated that JAK-mutated xenografts exhibited heightened activation status of JAK/STAT and MAPK signaling pathways compared with typical B-cell precursor ALL xenografts, which were inhibited by AZD1480 exposure. However, AZD1480 exhibited modest single-agent *in vivo* efficacy against JAK-mutated xenografts. Combining AZD1480 with selumetinib resulted in profound synergistic *in vitro* cell killing, although these results were not translated *in vivo* despite evidence of target inhibition. Despite validation of target inhibition and the demonstration of profound *in vitro* synergy between AZD1480 and selumetinib, it is likely that prolonged target inhibition is required to achieve *in vivo* therapeutic enhancement between JAK and MEK inhibitors in the treatment of JAK-mutated ALL. *Mol Cancer Ther; 14(2); 364–74. ©2014 AACR.*

Introduction

Although the overall cure rate for the most common pediatric cancer, acute lymphoblastic leukemia (ALL) now approaches 90%, certain high-risk subtypes experience shorter remission duration and a significantly reduced likelihood of survival (1). Recent genome-wide studies have focused on the molecular characterization of these high-risk subtypes, including B-cell precursor ALL (BCP-ALL) harboring mutations in the Janus kinases (JAKs; JAK-mutated ALL; refs. 2–4). Activating mutations in the pseudokinase or kinase domains of JAK1, JAK2, or JAK3 were detected in approximately 10% of high-risk pediatric ALL cases, and are frequently accompanied by deletion of the *IKZF1* gene. These cases also exhibit gene expression signatures similar to *BCR-ABL1*–positive ALL, despite the absence of *BCR-ABL1* translocations (2–4). The presence of JAK mutations in pediatric ALL with this "Kinase-like" gene expression signature is also significantly associated with high expression of cytokine receptor–like factor 2 (CRLF2) and a dismal outcome (2–4).

JAK mutations and CRLF2 overexpression result in aberrant activation of downstream signaling pathways, including JAK/STAT, MAPK, and PI3K/protein kinase B (PI3K/AKT) pathways (5–10). Cross-talk between the JAK/STAT, MAPK, and PI3K pathways has also been shown to occur at multiple levels (11). Constitutive activation of the JAK/STAT pathway enhances the MAPK and PI3K signaling pathways, causes cytokine-independent cell survival and proliferation of lymphoid cells (4, 5, 9, 12), and is implicated in the progression of lymphoproliferative diseases such as ALL, as well as other cancers (11, 13, 14). Consequently, they are compelling pathways for the development of targeted therapeutics to improve cancer treatment.

[1]Children's Cancer Institute Australia for Medical Research, Lowy Cancer Research Centre, University of New South Wales, Sydney, Australia. [2]Cancer Center, University of New Mexico, Albuquerque, New Mexico. [3]Department of Pathology, St. Jude Children's Research Hospital, Memphis, Tennessee. [4]Center for Childhood Cancer, Nationwide Children's Hospital, Columbus, Ohio. [5]Department of Biostatistics, St. Jude Children's Research Hospital, Memphis, Tennessee. [6]Department of Pediatrics, University of California at San Francisco, San Francisco, California. [7]University of Colorado Denver School of Medicine and Children's Hospital Colorado, Aurora, Colorado. [8]CTEP/NCI, Bethesda, Maryland.

Note: Supplementary data for this article are available at Molecular Cancer Therapeutics Online (http://mct.aacrjournals.org/).

S. Suryani and L.S. Bracken contributed equally to this article.

Corresponding Author: Richard B. Lock, Children's Cancer Institute Australia for Medical Research, Lowy Cancer Research Centre, University of New South Wales, PO BOX 81, Randwick, Sydney, New South Wales 2031, Australia. Phone: 1800-685-686; Fax: 612-9662-6583; E-mail: rlock@ccia.unsw.edu.au

doi: 10.1158/1535-7163.MCT-14-0647

Published OnlineFirst December 10, 2014; DOI: 10.1158/1535-7163.MCT-14-0647

Several small molecules with inhibitory activity against JAK family members have shown preclinical and clinical activity in the treatment of myeloproliferative neoplasms, which harbor the JAK2 V617F mutation, as well as other solid tumors (15–20). Although the JAK2 V617F mutation is different from those that occur in ALL, these mutations occur in the same region of the protein and are functionally analogous *in vitro* (4, 5). AZD1480 is an ATP-competitive small-molecule inhibitor of JAK1 and JAK2 that also shows some selectivity towards JAK3 (20, 21). AZD1480 was selected by the Pediatric Preclinical Testing Program (PPTP) for preclinical efficacy testing against a panel of xenografts established in immunodeficient mice that were derived from high-risk pediatric ALL patient subtypes, including those harboring JAK point mutations, JAK2 fusions, high CRLF2 expression, and a Kinase-like gene expression profile. This rationale was based on the success achieved with imatinib in the treatment of *BCR-ABL1*–positive leukemia (22).

The JAK1/2 inhibitor ruxolitinib was recently shown to exhibit greater *in vivo* efficacy against two Kinase-like pediatric ALL patient-derived xenografts with activation of the JAK/STAT axis (one via a *BCR-JAK2* translocation) but without CRLF2 overexpression, compared with several xenografts derived from Kinase-like cases harboring JAK point mutations and CRLF2 overexpression (23). This observation suggests that alternative survival pathways activated by CRLF2 may result in reduced sensitivity of ALL cells with activated JAK/STAT signaling to single-agent JAK inhibitors. Therefore, because xenografts established from JAK-mutated/CRLF2-high ALL biopsies would also be expected to exhibit heightened activation of the MAPK and PI3K/AKT pathways in addition to JAK/STAT (4, 5, 9, 12), we sought to enhance antileukemic efficacy by targeting multiple signaling nodes using the combination of AZD1480 and the MEK inhibitor, selumetinib (AZD6244, ARRY-142886). Selumetinib is a potent small-molecule inhibitor of MEK1/2, which blocks ERK1/2 activation (24). Despite strong evidence of *in vitro* synergy between AZD1480 and selumetinib, both drugs exhibited modest *in vivo* single-agent and combination efficacy. These findings highlight the complexity of translating *in vitro* synergistic drug combinations to the *in vivo* setting, and suggest that prolonged target inhibition may be required to achieve *in vivo* therapeutic benefit using JAK inhibitors for the treatment of pediatric ALL cases harboring JAK point mutations and high CRLF2 expression.

Materials and Methods

Patient and xenograft details

Pretreatment leukemia specimens were obtained from 21 children with high-risk BCP-ALL enrolled in the Children's Oncology Group (COG) P9906 clinical trial, and were molecularly characterized by the Therapeutically Applicable Research to Generate Effective Treatments (TARGET) initiative (Table 1; ref. 3). Procedures by which continuous xenografts are routinely established from childhood ALL biopsies in female 6–8 week old 20–25 g immunodeficient NOD/SCID (NOD.CB17-Prkdc^{scid}/SzJ) or NOD/SCID/IL-2 receptor gamma$^{-/-}$ (NOD.Cg-Prkdc^{scid} Il2rg^{tm1Wjl}/SzJ, NSG) mice, and criteria for determining successful engraftment, have been described in detail previously (25–27). Additional established BCP-ALL (ALL-4, ALL-10$^{JAK1/V658L}$, ALL-19, ALL-25 and ALL-26) and T-ALL (ALL-31) xenografts were included in this study (26). JAK mutations are detailed where annotated.

Affymetrix U133_Plus_2.0 expression arrays

RNA from 38 xenograft samples was isolated from cryopreserved cells, labeled, and hybridized to Affymetrix U133_Plus_2.0 arrays as previously described (2). These new data, and the 13 parental samples analyzed in our prior study, were also masked and normalized by MAS5 as previously reported (2). The gene expression dataset can be accessed via Gene Expression Omnibus (http://www.ncbi.nlm.nih.gov/geo) under accession numbers GSE11877 and GSE58290. The xenograft samples were scanned in 2011, whereas the parent samples were scanned in 2006. The results for the 3 microarray quality control inclusion criteria are provided in Supplementary Table S1. Samples were retained only if all 3 conditions were satisfied: scale factors <35; GAPDH 3′ signal for M33197 >15,000; and, the GAPDH 3′:5′ ratio < 3.5. All but one of the xenografts (XRL_24) met these conditions.

Of the 54,675 probe sets on the Affytmetrix U133_Plus_2.0 array, 89 represent X- and Y-specific transcripts associated with sex, 62 are Affymetrix controls, and 20 are globins. Removal of these resulted in 54,504 potentially informative probe sets. The average median expression across all the arrays was 173. A minimally interpretable expression level of 500 (~3-fold background) was established and all values <500 were set to a baseline of 500 for subsequent analysis. A total of 18,090 probe sets (33.2%) showed no signals greater than this baseline for any of the samples, leaving 36,414 probe sets for a comparison of xenografts to parental samples.

Quantitative RT-PCR

One microgram of total RNA was converted to cDNA using the High Capacity cDNA kit (Life Technologies). This was diluted to 50 μL and mixed with an equal volume of TaqMan Universal Master Mix II without UNG (Life Technologies). The 24 genes and an endogenous control gene (*EEF2*) were selected from the group of inventoried assays (available upon request) and were plated on custom microfluidic cards (Life Technologies). The sample ports were filled with the cDNA/master mix and the cards were sealed and run on an ABI model 7900HT instrument using the following parameters: 94.5°C for 10 minutes followed by 40 cycles of 97.0°C for 30 seconds and 59.7°C for 1 minute. A manual C_t threshold of 0.2 and automatic baseline were applied as analysis settings. The raw C_t value for the endogenous control sample, *EEF2*, was required to be <30. The ΔC_t values were calculated by subtracting the *EEF2* C_t from each gene's C_t. Even though most samples had *EEF2* C_t values much less than 30, a maximum ΔC_t of 10 was applied to all gene intensities to permit equivalent treatment across all samples.

Statistical and analytical software

Affymetrix microarray data were analyzed using Expression Console (build 1.3.0.187, Affymetrix). Microfluidic cards were analyzed using SDS 2.4.1 software (Life Technologies). Heatmaps were created using MATLAB and its Bioinformatics toolbox (R2013b; MathWorks).

In vitro culture and drug treatments

Xenograft cells were retrieved from cryostorage and resuspended in QBSF-60 medium (Quality Biological) supplemented with Flt-3 ligand (20 ng/mL), penicillin (100 U/mL), streptomycin (100 μg/mL), and L-glutamine (2 mmol/L). Viability was determined by Trypan blue exclusion. Before treatment, cells were plated in 96-well plates (100 μL/well) at a density previously

Published OnlineFirst December 10, 2014; DOI: 10.1158/1535-7163.MCT-14-0647

Table 1. Primary patient biopsy, ALL xenograft genotypes and *in vitro* and *in vivo* responses to AZD1480

Xenograft		*CRLF2* status		Kinase-like	Other kinase lesions	Alteration in B-cell genes and *CDKN2A/B*	Sample origin	Number of mice inoculated	Number of mice engrafted	Continuous xenograft	*In vivo* AZD1480		*In vitro* AZD1480
ID	*JAK* status	Expression	Rearrangement								LGD	ORM	IC_{50} (μmol/L)
PAMDKS	JAK2 R683G	High	*IGH@-CRLF2*	Yes		*IKZF1, PAX5, CDKN2A*	PB	7	2	No			
PALKTY	JAK2 2GinsR683	High	*P2RY8-CRLF2*	Yes		*IKZF1, CDKN2A/B*	PB	5	4	No			
PAKRSL	JAK2 R683G	High	*IGH@-CRLF2*	Yes		*IKZF1, CDKN2A/B*	PB	7	7	Yes	0.0	PD1	>10
PALJCF	JAK1 L624_R629>W	High	*P2RY8-CRLF2*	Yes		*CDKN2A/B*	BM	5	3	Yes	−3.1	PD1	>10
PALTIC	JAK2 D873N	High	*P2RY8-CRLF2*	Yes		*IKZF1, PAX5*	BM	4	0	No			
PAKHZT	JAK2 R867Q	High	*IGH@-CRLF2*	Yes		*CDKN2A/B*	PB	6	3	Yes	12.7	PD2	0.9
PAKMZM	JAK2 I682F	High	*IGH@-CRLF2*	Yes		*IKZF1, PAX5, CDKN2A*	PB	8	4	No			
PAKSWW	JAK1 V658F	High	*IGH@-CRLF2*	Yes			PB	8	8	Yes	−11.3	PD1	5.0
PALLSD	JAK2 R683G	High	*IGH@-CRLF2*	Yes		*IKZF1, PAX5, CDKN2A*	BM	2	2	Yes	0.0*	PD1[a]	>10
PALNTB	JAK2 P933R	High	*IGH@-CRLF2*	No		*IKZF1, CDKN2A/B*	BM	7	7	Yes	−0.5	PD1	>10
PAMDRM	JAK2 GPinsI683	High	*IGH@-CRLF2*	Yes		*IKZF1, EBF1, PAX5, CDKN2A/B*	BM	6	6	Yes	10.0[a]	PD1[a]	>10
PAKMVD	JAK1 S646F	Normal		Yes		*PAX5, CDKN2A*	PB	3	0	No			
PAKGHN	JAK3 S789P	Normal		Yes		*EBF1*	BM	8	0	No			
PAKKXB	Wild-type	High	*IGH@-CRLF2*	Yes		*IKZF1, CDKN2A/B*	PB	4	2	No			
PALTWS	Wild-type	High	*IGH@-CRLF2*	No		*IKZF1, PAX5, CDKN2A*	BM	12	12	Yes			
PAKKCA	Wild-type	Normal		Yes	*EBF1-PDGFRB*	*IKZF1, CDKN2A/B, PAX5*	BM	4	1	No			
PALIBN	Wild-type	Normal		Yes	*IGH@-EPOR*	*IKZF1, CDKN2A/B*	BM	8	0	No			
PALJDL	Wild-type	Normal		Yes	*IL7R, SH2B3*	*PAX5, CDKN2A*	BM	10	9	Yes	11.6	PD2	2.4
PAKVKK	Wild-type	Normal		Yes	*NUP214-ABL1*	*IKZF1, PAX5, CDKN2A*	PB	10	9	Yes			
PAKYEP	*BCR-JAK2*	Normal		Yes		*IKZF1, PAX5, CDKN2A*	BM	7	3	Yes	9.3	PD2	1.3
PAKTAL	*STRN3-JAK2*	Normal		Yes		*IKZF1, PAX5*	BM	7	0	No			
ALL-4	Wild-type	Normal			*BCR-ABL1*		NA	NA	NA	Yes	0.6	PD1	
ALL-10	JAK1 V658L	High		Yes			NA	NA	NA	Yes	3.4	PD2	0.6
ALL-19	Wild-type	Normal					NA	NA	NA	Yes			
ALL-25	Wild-type	Normal					NA	NA	NA	Yes			
ALL-26	Wild-type	Normal				*ETV6-RUNX1*	NA	NA	NA	Yes			
T-ALL-31	Wild-type	Normal					NA	NA	NA	Yes	−1.1	PD1	>10

Abbreviations: BM, bone marrow; LGD, leukemia growth delay; NA, not applicable; ORM, objective response measure; PB, peripheral blood; PD, progressive disease.

[a]Values shown are AZD1480 single agent as part of the AZD1480/AZD6244 combination study. The dose was attenuated to 30 mg/kg twice daily Monday to Friday for 2 weeks.

Published OnlineFirst December 10, 2014; DOI: 10.1158/1535-7163.MCT-14-0647

optimized (3–6 × 10^6/mL) and equilibrated overnight at 37°C in 5% CO_2. Cells were exposed to 10-fold serial dilutions of AZD1480 or selumetinib (AstraZeneca; 10^{-6} to 10^{-12} mol/L) for 72 hours, following which AlamarBlue reagent (Life Technologies) was added and fluorescence was measured at 0, 6, and 24 hours using a fluorescent plate reader (VICTOR^3; PerkinElmer; excitation 560 nm, emission 590 nm). For fixed ratio combination assays, cells were treated with AZD1480 and selumetinib, alone or in combination, at 4, 2, 1, 0.5, 0.25, and 0.1 μmol/L. The combination drug effect was assessed using Calcusyn software (Version 2.0, Biosoft) to calculate combination indices (CI) indicative of synergy (CI < 1), additivity (CI = 1), or antagonism (CI > 1).

In vivo drug treatments

AZD1480 and selumetinib were obtained from AstraZeneca under a standard Materials Transfer Agreement. Structures of both drugs are shown in Supplementary Fig. S1. Groups of 8 to 10 mice were inoculated with 5 × 10^6 xenograft cells retrieved from cryostorage, and engraftment monitored by weekly enumeration of the proportion of human $CD45^+$ cells in the peripheral blood (%$huCD45^+$; refs. 26, 27). Drug treatments were initiated when the median %$huCD45^+$ exceeded 1% for each cohort. For single-agent *in vivo* efficacy testing, AZD1480 was administered by oral gavage twice daily at 10 mg/kg for 5 days, followed by a single daily dose of 15 mg/kg for 2 days. This cycle was repeated 3 times. For the combination efficacy study selumetinib (25 mg/kg) was administered 3 hours before AZD1480 (30 mg/kg), and both drugs were administered once daily by oral gavage Monday to Friday for 2 weeks and were dissolved in 0.5% hydroxypropyl methylcellulose and 1% Tween-80, with the pH adjusted to 3.0 for AZD1480. A preliminary tolerability study on nonengrafted mice had shown that this was the maximum tolerated dose and schedule of the combined drugs.

Following randomization of mice and the initiation of drug treatment, the %$huCD45^+$ was measured weekly. Individual mouse event-free survival (EFS) was calculated as the day from treatment initiation until the %$hCD45^+$ reached 25%. The EFS was represented graphically by Kaplan–Meier analysis and survival curves were compared by log-rank test. The efficacy of the drug treatment was evaluated by leukemia growth delay (LGD), calculated as the difference between the median EFS of the drug-treated cohort and the median EFS of the vehicle-treated cohort. An objective response measure (ORM), modeled after stringent clinical criteria, was assigned to individual mice, which allowed the determination of a median group response as described previously (25). Detailed methodology is presented in the Supplementary Methods and Supplementary Table S2. Correlations between *in vivo* and *in vitro* drug sensitivity were assessed by Spearman test. To evaluate interactions between drugs *in vivo*, Therapeutic Enhancement was defined as the EFS of mice treated with the drug combination being significantly greater than both single agents used at their maximum tolerated doses (28, 29).

Analysis of protein expression

Methods for preparation of whole-cell extracts, determination of protein concentrations, and analysis of cellular proteins by immunoblotting have been described in detail elsewhere (30). Antibody details can be provided upon request. Ba/$F3^{TEL\text{-}JAK2}$–positive control cells were kindly provided by Dr. Chris Burns (Walter and Elisa Hall Institute of Medical Research, Melbourne, Victoria, Australia).

In vivo pharmacodynamic analysis

Mice were inoculated with PAMDRM xenograft cells, and monitored until the %$hCD45^+$ reached ≥25%. The following treatment was administered with three mice per group per time-point: (i) vehicle control; (ii) one dose of AZD1480 (30 mg/kg); (iii) one dose of selumetinib (25 mg/kg); and (iv) one dose of selumetinib (25 mg/kg) 3 hours before one dose of AZD1480 (30 mg/kg). Spleen, peripheral blood (PB), and bone marrow (BM) samples were collected at 2 and 9 hours post-AZD1480 treatment for phosphorylated protein analysis by immunoblotting as described above.

Results

Development and characterization of xenografts derived from JAK-mutated pediatric ALL biopsies

Of the original 21 bone marrow or peripheral blood biopsy specimens inoculated from the P9906 study, 15 showed evidence of engraftment in at least 2 mice using previously defined criteria (Table 1; ref. 27). This engraftment efficiency was lower than expected (27), and closer inspection revealed a distinct relationship between high CRLF2 expression and engraftment potential in this subset of high-risk ALL samples (Supplementary Fig. S2). The proportion of mice engrafted with CRLF2 high samples was significantly greater than CRLF2 normal samples ($P = 0.023$). Similarly, higher levels of spleen ($P = 0.036$), peripheral blood ($P = 0.043$), and bone marrow ($P = 0.019$) infiltration were observed in the CRLF2 high compared with CRLF2 normal xenografts. The gene expression profiles of spleen-derived cells from primary xenografts of 37 mice representative of 13 patient samples were then analyzed in relation to the original biopsy (parental) specimen.

Supplementary Table S1 lists the 13 parent samples and their corresponding xenografts analyzed at first passage. In addition, partial clinical information on the underlying lesions in the parental sample is provided in Table 1. The lesions and mutations of these parental samples have been previously characterized and reported as part of a larger study by Roberts and colleagues (6). Eleven of the 13 parents have *CRLF2* lesions (9 *IGH-CRLF2* and 2 *P2RY8-CRLF2*) with all but one of these (PALTWS) also having a *JAK* mutation. Each of the two cases without a *CRLF2* lesion has a different kinase-related lesion (*NUP214-ABL1* or *IL7R* mutation with *SH2B3* deletion). Overall, eleven of the 13 parents also are considered Kinase-like on the basis of their gene expression pattern. The two primary leukemias that are not Kinase-like (PALNTB and PALTWS) both have *IGH–CRLF2* translocations.

Overall, the quality of the xenograft samples was much better than the parent samples for scale factor and *GAPDH* expression: median xenograft scale factor 6.0 v. 15.9 and median *GAPDH* 63,272 v. 49,762 for the xenografts and parents, respectively (Supplementary Table S1). The median 3′:5′ ratios were comparable for the parents and xenografts (1.2 and 1.3, respectively; Supplementary Table S1). Despite the 5-year gap between analyzing the parent and xenograft samples, and the different lots of materials, there appeared to be no obvious large differences in the arrays. Supplementary Fig. S3 shows the distribution of expression levels for the 54,504 probe sets across all the parent samples

Published OnlineFirst December 10, 2014; DOI: 10.1158/1535-7163.MCT-14-0647

and xenografts. Overall, 89.7% of these intensities were less than 1,500 (3-fold baseline). For the purposes of comparing xenograft expression to the parental lines, only those probe sets with parental expression >1,500 (9,741 of 54,504 probe sets) were evaluated, which permitted a minimum interpretation of 3-fold higher or lower expression. There were 2,052 of 9,741 probesets (21.1%) with expression levels >1,500 in all 13 of the parent samples. Each of the 37 xenograft samples was compared with its parent sample and the concordance of expression was evaluated. The number of interpretable probe sets (expression >1,500) for each of the 13 parent samples ranged from 3,911 to 5,671 (median 5,221; mean 5,127). Concordance of each of the xenografts was determined by whether the expression for these probe sets in the xenografts was within three-fold of its parent expression. The overall frequency of xenograft expression within three-fold of parental expression for the interpretable probe sets is shown in Supplementary Table S3 and ranged from 74.2% to 95.0% (median 84.1%; mean 84.0%). Supplementary Table S3 also shows the R-squared (RSQ) results and slope for the correlation between the intensities of parent samples with the xenografts. RSQ values ranged from 0.644 to 0.901 (median 0.831; mean 0.820) and the slopes varied from 0.385 to 1.306 (median 0.835; mean 0.817).

We also explored the possibility that certain probe sets would be uniquely associated with either the parent or xenograft material. Probe sets were selected on the basis of the minimum expression by type (either parent or xenograft) being higher than the maximum expression of the alternative type. They were also required to have the average expression for the higher expressing category >1,500. Supplementary Tables S4 and S5 show the probe sets identified by this approach. Only 20 probe sets were found in which the expression of the parents was always higher than the xenografts (Supplementary Table S4). A similar result was obtained for probe sets in which the xenograft expression always exceeded the parents ($n = 26$, Supplementary Table S5). For the most part, these probe sets were differentially expressed rather than being completely on or off. The most noteworthy exceptions are 217572_at and 231628_s_at. For these two probe sets the parent samples had no detectable expression (baseline of 500), whereas the average xenograft expression was 75,903 and 23,880, respectively.

Given the emphasis on *CRLF2* lesions (and underlying *JAK* mutations) in the selection of the parents of the xenografts, we also wanted to see how well the xenografts retained the parental expression of *CRLF2*. Eleven of the 13 parental samples had *CRLF2* lesions (9 with *IGH-CRLF2* and 2 with *P2RY8-CRLF2*) and originally showed high *CRLF2* expression. All xenografts for these 11 cases had expression levels >1,500 and ranged from 0.58 to 3.31 times the parental intensity (median 1.28; mean 1.48).

In addition to the comparison of array data, qRT-PCR for a panel of 24 genes that were previously shown to be differentially expressed in a cohort of patients with ALL (2, 6) was also performed (Fig. 1). Nearly all of the genes showed comparable expression levels for their respective xenografts. The most notable exception to this is sample PAKSWW, for which 3 xenografts are shown. All 3 of the xenografts display nearly identical expression levels, yet none of these retain the relatively high *IGJ* expression of the parent. A heatmap of the microarray gene expression data is shown in Supplementary Fig. S4, which corresponds to the qRT-PCR data shown in Fig. 1.

Continuous xenografts have been established from 11 of the 15 primary xenografts following inoculation of spleen-derived cells into secondary and tertiary recipient mice (Table 1). Spleen-derived cells from these secondary and/or tertiary engrafted mice were used in the experiments described below.

AZD1480 inhibits aberrant JAK/STAT signaling in JAK-mutated xenografts

Because previous studies have shown that JAK mutations result in aberrant signaling via the JAK/STAT, MAPK, and PI3K/AKT pathways (2–5, 14, 31), we analyzed basal expression levels of key phosphoproteins as a surrogate for pathway activation in the xenograft panel. JAK-mutated xenografts exhibited increased signaling in JAK/STAT, MAPK, and PI3K/AKT signaling relative to xenografts ALL-25 and ALL-26, which have no annotated JAK mutations, as shown by elevated levels of pJAK1, pJAK2, pSTAT1, pSTAT3, pSTAT5, pMEK1/2, and pAKT (Fig. 2A). Elevated levels of these phosphoproteins were not uniform across all JAK-mutated xenografts.

The ability of AZD1480 to inhibit JAK/STAT signaling was tested across three JAK-mutated xenografts (PAKHZT, PAKRSL, and PALNTB) and compared with a xenograft harboring an activating translocation in JAK2 (BCR-JAK2, PAKYEP), as well as a xenograft with lesions in *IL7R* and *SH2B3* (PALJDL). AZD1480 broadly decreased levels of pSTAT1/3/5 across the xenografts (Fig. 2B). In contrast, AZD1480 had minimal effects on pMEK1/2 and pAKT levels in all xenografts with the exception of PALJDL, which showed decreased levels of these phosphoproteins. Phosphorylation of ERK1/2 was also reduced in 3 of 5 xenografts tested (PAKHZT, PAKRSL, and PALJDL).

AZD1480 exerts variable antileukemic efficacy *in vitro* and *in vivo*

To gain additional evidence for the use of JAK inhibitors such as AZD1480 for the treatment of patients with JAK-mutated ALL, we tested its *in vitro* and *in vivo* efficacy against representative xenografts. The *in vitro* IC_{50} values for xenografts ranged from 0.6–5.0 μmol/L for 5 xenografts, to >10 μmol/L for the remaining 6 tested (Table 1; Fig. 2C and D and Supplementary Fig. S5). The 5 most sensitive xenografts (PAKHZT, PAKSWW, PAKYEP, PALJDL, and ALL-$10^{JAK1/V658L}$), including that with *BCR-JAK2* fusion (PAKYEP) and wild-type JAK (PALJDL), did not appear to conform to any specific JAK mutational status. Moreover, the differences in AZD1480 *in vitro* sensitivity did not appear to relate to differential inhibition of the JAK/STAT and MAPK signaling pathways, as described above and in Fig. 2B.

When tested *in vivo* as a single-agent AZD1480 induced significant progression delays in 3 of 10 of the JAK-mutated xenografts (Table 1; Fig. 3, Supplementary Table S6 and Supplementary Fig. S6). Despite some evidence of activity in delaying leukemia progression, AZD1480 was unable to elicit objective responses (modeled after stringent clinical criteria) in any of the xenografts regardless of their JAK status (all were scored as Progressive Disease, PD1 or PD2). A complete summary of results is provided in Table 1, Supplementary Tables S6 and S9, including total numbers of mice, number of mice that died (or were otherwise excluded), numbers of mice that reached event, average time to event, LGD values, as well as numbers in each of the ORM categories and median ORM values.

Published OnlineFirst December 10, 2014; DOI: 10.1158/1535-7163.MCT-14-0647

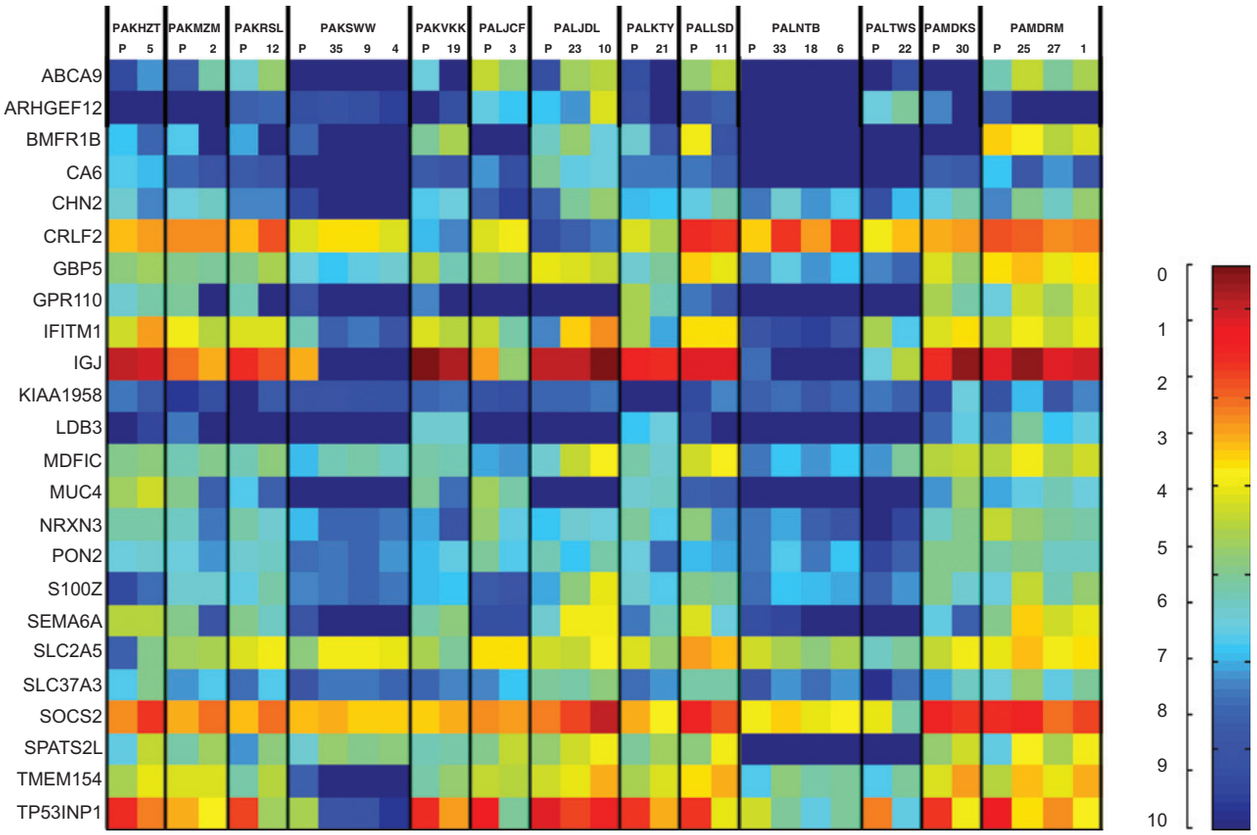

Figure 1.
Expression of candidate genes in xenografts and parent samples. qRT-PCR ΔC_t data for parental samples and representative xenografts are shown for 24 selected genes. The color scale spans a 1,024-fold range of expression with each unit representing a doubling in intensity. At the high end of the scale, the darkest red indicates expression at the same level as *EEF2* (the control gene, $\Delta C_t = 0$), while the darkest blue denotes expression at least 10-doublings lower ($\Delta C_t = 10$). The minimum expression value for any gene is 10. Numbers above columns refer to unique xenograft identifiers, and correspond to those listed in Supplementary Tables S1 and S3. P, parental sample.

Rational targeting of the JAK/STAT and MAPK pathways to achieve synergistic antileukemic efficacy

Because of the modest single-agent activity exhibited by AZD1480 *in vitro* and *in vivo*, we investigated the potential for combination with other pathway inhibitors. As JAK-mutated ALL cells and JAK wild-type with a Kinase-like signature exhibited aberrant JAK/STAT and MAPK signaling (Fig. 2A and B), but modest inhibition of MAPK signaling by AZD1480 alone (Fig. 2B), we tested the combination of AZD1480 with selumetinib. Fixed ratio *in vitro* cytotoxicity assays revealed that the AZD1480/selumetinib combination exerted strong to very strong synergistic effects in 4 of 5 JAK-mutated ALLs (PAKRSL, PALJCF, PALLSD, and PAMDRM; average CI values < 0.14; Fig. 4A–D and J, Supplementary Table S7). Synergism and moderate synergism were also observed with ALL-$10^{JAK1/V658L}$ (CI = 0.34) and PALJDL (CI = 0.73), respectively (Fig. 4E and I and Supplementary Table S7). In contrast, antagonism was observed for ALL-4, ALL-19 and ALL-26 (CI values > 1; Fig. 4F–H and J and Supplementary Table S7). Significantly greater synergy between AZD1480 and selumetinib was observed in the JAK-mutated compared with the JAK wild-type xenografts ($P = 0.036$; Fig. 4K). Of note, selumetinib alone exhibited poor single-agent activity against all xenografts tested (IC_{50} >10 μmol/L; Fig. 4A–I), regardless of their JAK mutational status.

The combined effects of AZD1480 and selumetinib were also assessed by phosphoprotein analysis of the PALLSD and PAMDRM xenografts. Consistent with the results presented in Fig. 2B, AZD1480 alone markedly decreased STAT1/3/5 phosphorylation (Fig. 4L and M). Selumetinib alone exerted minimal effects on levels of phosphorylated STATs, but substantially decreased pERK1/2 levels in both xenografts. Reduced levels of pSTAT1/3/5 and pERK1/2 were maintained or even enhanced with combination treatment for up to 24 hours in both xenografts. Minimal changes in pAKT were observed throughout the 24-hour treatment period for both xenografts.

Because of the strong synergy observed between AZD1480 and selumetinib against JAK-mutated xenografts *in vitro*, the combination was tested *in vivo* against xenografts PALLSD and PAMDRM, which both exhibited very strong synergism *in vitro* (Supplementary Table S7). Although AZD1480 alone delayed the progression of PAMDRM by 10 days, it did not delay the leukemia progression of PALLSD with both responses categorized as PD1 (Fig. 5A and B, Table 1; Supplementary Tables S8–S9). Selumetinib alone exerted no significant antileukemic efficacy against either xenograft. Despite the combination of AZD1480 and selumetinib exerting a significant progression delay in PAMDRM in comparison with vehicle-treated control and selumetinib alone, no objective responses or Therapeutic Enhancement were

Published OnlineFirst December 10, 2014; DOI: 10.1158/1535-7163.MCT-14-0647

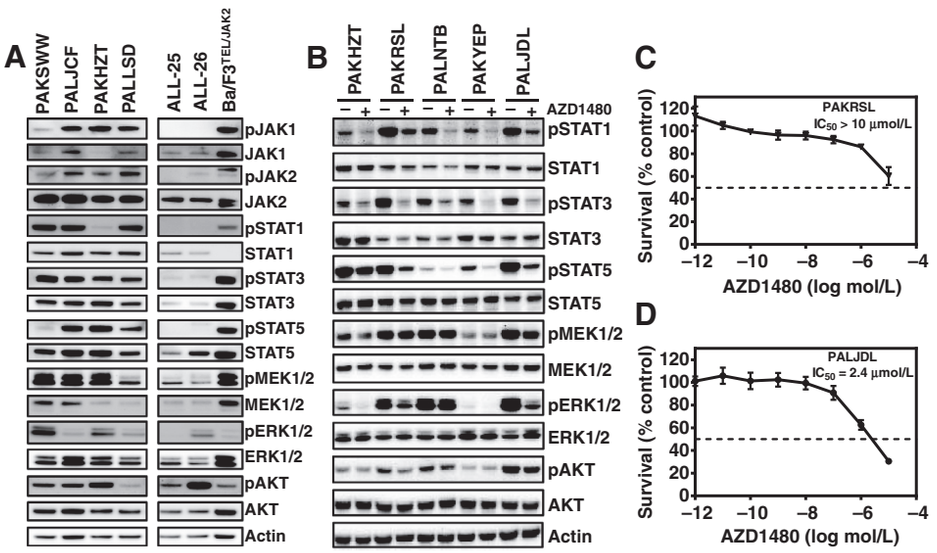

Figure 2.
Aberrant signaling pathways in JAK-mutated xenografts and their inhibition by AZD1480. A, immunoblots of signaling proteins involved in the JAK/STAT, MAPK, and PI3K/AKT pathways in a panel of JAK-mutated and JAK wild-type xenografts. Ba/F3$^{TEL-JAK2}$ cells were included as positive controls. B, effects of *in vitro* AZD1480 treatment (1 μmol/L, 1 hour) on signaling proteins in JAK mutated and JAK wild-type with a kinase-like signature xenograft cells. C and D, *in vitro* sensitivity of xenograft cells to single-agent AZD1480. Representative cytotoxicity curves of a resistant (PAKRSL, C) and sensitive (PALJDL, D) xenograft are shown. Following exposure of cells to various AZD1480 concentrations for 72 hours, viability was determined by AlamarBlue assay. Each data point represents the mean ± SEM of 3 independent experiments.

observed. A complete summary of all *in vivo* results is provided in Supplementary Tables S6, S8, and S9.

Pharmacodynamic evaluation of AZD1480 and selumetinib in leukemia-engrafted mice

In an effort to understand our inability to translate the profound *in vitro* synergistic interactions between AZD1480 and selumetinib to the *in vivo* setting, we evaluated signaling pathways by phosphoprotein immunoblots of PAMDRM cells harvested from the spleens of highly engrafted mice following drug treatment. Although both drugs alone and in combination profoundly reduced pSTAT1/3/5, and pERK1/2 levels at 2 hours after treatment (Fig. 5C), all had recovered to control levels by 9 hours. Moreover, although pAKT levels were not affected at 2 hours after treatment, they had increased markedly at 9 hours in the AZD1480 and combination-treated mice relative to control levels. Subsequent reassessment of the *in vitro* combination cytotoxicity assays revealed that, whereas the length of drug exposure did not substantially affect the activity of the single agents, the profound synergy observed between AZD1480 and selumetinib against PALLSD and PAMDRM required continuous drug exposures in excess of 12 hours (Supplementary Fig. S7). Moreover, 72-hour exposure of PAMDRM cells to the AZD1480/selumetinib combination resulted in a greater repression of pSTAT1/3/5, pAKT, and pERK compared with cells only treated for 12 hours (Supplementary Fig. S8), further supporting the requirement for prolonged pathway inhibition to achieve synergistic cytotoxicity.

Discussion

Patient-derived xenografts are increasingly recognized as important tools for understanding tumor biology and optimizing new treatments. This study describes the development and molecular characterization of a large panel of xenografts derived from a cohort of high-risk patients with Kinase-like gene expression signatures, most of which harbor JAK mutations. The concordance in gene expression profiles between xenografts and parent biopsies is remarkable, considering the number of uncontrollable variables associated with analysis of the batches of samples several years apart, indicating that these xenografts provide a valuable resource for preclinical experimental therapeutics.

Previous reports have identified dysregulation of multiple key signaling pathways in Kinase-like ALL (6, 13), while Tasian and colleagues reported that both JAK/STAT and PI3K/mTOR pathways are activated in CRLF2-rearranged BCP-ALL (9). The JAK-mutated ALL xenografts established in this study also exhibited constitutive activation of JAK/STAT, MAPK, and PI3K/AKT pathways in contrast to BCP-ALL xenografts. Thus, the expectation was that pharmacologic inhibition of the JAK/STAT pathway with AZD1480 in JAK-mutated xenografts would result in substantial *in vitro* and *in vivo* antileukemic efficacy. However, despite evidence that AZD1480 inhibited JAK/STAT signaling both *in vitro* and *in vivo*, it exerted modest antileukemia efficacy and significantly delayed the progression of only 3 of 10 xenografts *in vivo*. With the exception of one xenograft with BCR-JAK2 fusion (PAKYEP) and one xenograft with JAK wild-type (PALJDL), the extent of leukemia progression is consistent with that reported for the JAK1/2 inhibitor ruxolitinib against JAK-mutated ALL xenografts (6, 23). Previously, significant decreases in leukemia burden were observed when mice engrafted with PAKYEP and PALJDL were treated with ruxolitinib (23). One possible explanation for the difference in efficacy between the two studies is that ruxolitinib was administered by continuous subcutaneous infusion, while we administered AZD1480 by oral gavage once or twice daily. As demonstrated in this study, the inhibitory effects of 10 mg/kg AZD1480 lasted between 2 and 9 hours *in vivo*.

Published OnlineFirst December 10, 2014; DOI: 10.1158/1535-7163.MCT-14-0647

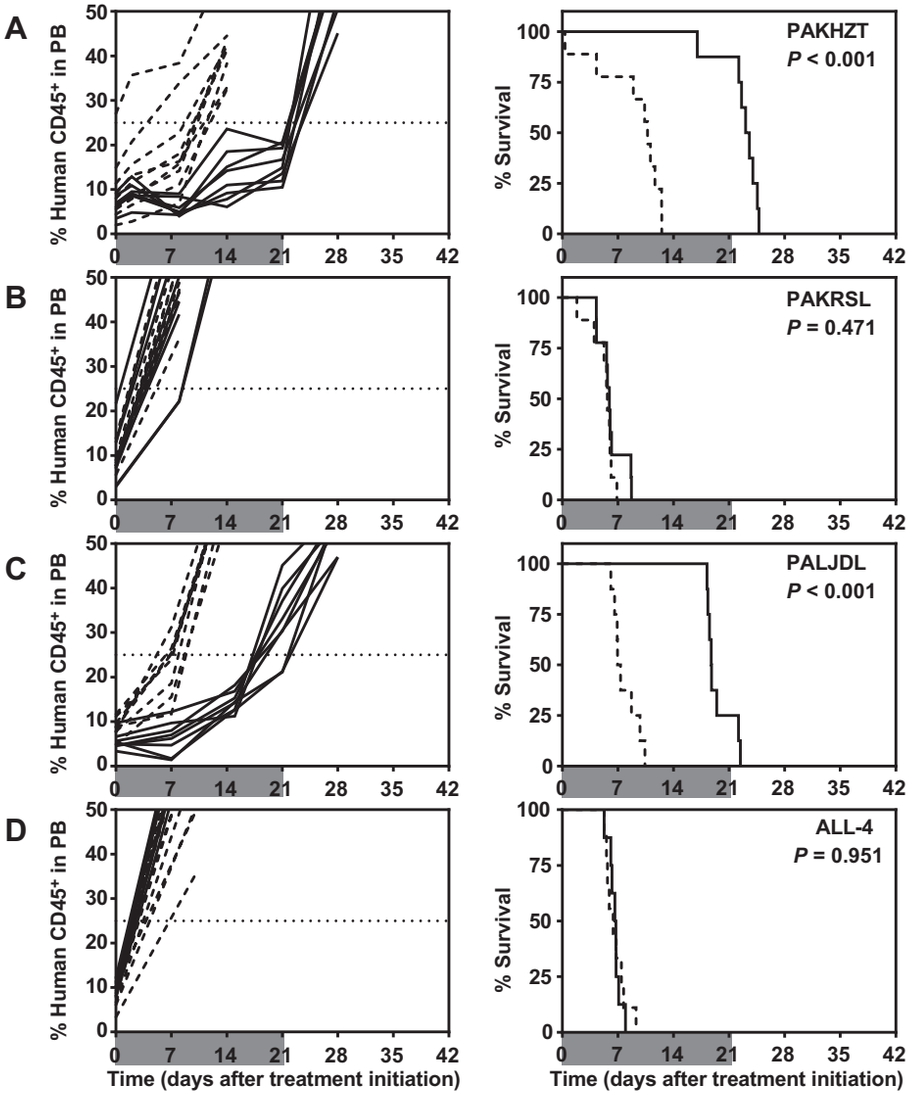

Figure 3.
In vivo sensitivity of representative ALL xenografts to AZD1480. The panel illustrates the *in vivo* AZD1480 responses of two JAK-mutated (A and B) and two JAK wild-type (C and D) xenografts. Results are presented as the percentage of huCD45$^+$ cells in the PB over time (left) or mouse EFS (right). Gray shading indicates the treatment period. Dashed lines, vehicle control–treated mice; solid lines, AZD1480-treated mice. Log-rank *P* values are shown comparing control and treated for each xenograft.

Therefore, the lack of any observed objective responses in the current study when stringent objective response criteria developed by the Pediatric Preclinical Testing Program (25) were applied indicates that prolonged target inhibition is likely to be required to achieve significant therapeutic benefit. Furthermore, the apparent increased sensitivity of xenografts PAKYEP and PALJDL to both ruxolitinib and AZD1480 *in vivo* suggests that Kinase-like ALL cells with normal CRLF2 expression are more dependent on the JAK/STAT pathway than those with JAK point mutations and high CRLF2 expression.

Recent reports have highlighted compensatory activation of signaling pathways in response to inhibition of a single kinase node, and the successful targeting of dual pathways to achieve therapeutic synergy (32–34). Therefore, we explored dual inhibition of the JAK/STAT and MEK pathways in JAK-mutated ALL xenografts to improve the *in vitro* and *in vivo* antileukemic efficacy of a JAK inhibitor when used alone. We observed potent synergistic cell killing *in vitro* with the AZD1480/selumetinib combination at submicromolar concentrations, suggesting that both the JAK/STAT and MAPK pathways are critical for the survival of JAK-mutated ALL. There was also evidence for selectivity in this synergy against JAK-mutated/Kinase-like xenografts, as synergy was not observed in 4 xenografts with wild-type JAK (Fig. 4J). However, despite the AZD1480/selumetinib combination significantly delaying the progression of one JAK-mutated xenograft, no objective responses were achieved. These results, along with our additional *in vitro* combination cytotoxicity experiments and pharmacodynamics study, suggest that prolonged pathway inhibition is required in order to achieve synergy between AZD1480 and selumetinib.

The plasma half-life ($t_{1/2}$) of AZD1480 was approximately 2 and 5 hours in mouse models (21) and humans (35), respectively. However, whereas the human study showed maximal pSTAT inhibition in circulating granulocytes at 1 to 2 hours postadministration (35), a murine Ba/F3 TEL-JAK2 model showed prolonged pSTAT5 inhibition for up to 12 hours in spleen-derived cells upon administration of a 30 mg/kg dose, consistent with significant *in vivo* antileukemic efficacy (21). In the same study, pSTAT5 suppression was observed to a maximum of 8 hours at the 10 mg/kg dose, consistent with our findings. The $t_{1/2}$

Published OnlineFirst December 10, 2014; DOI: 10.1158/1535-7163.MCT-14-0647

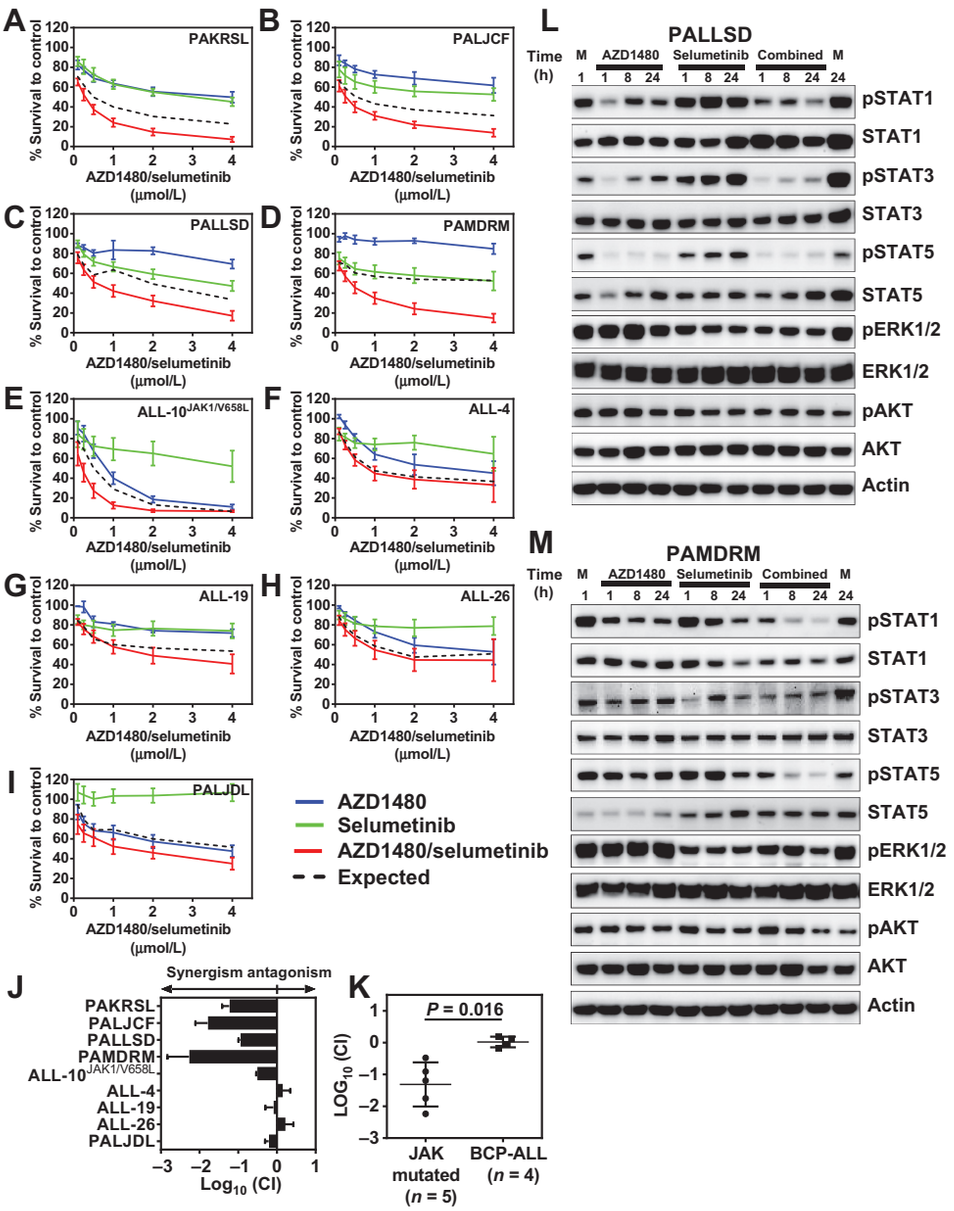

Figure 4.
Combination effects of AZD1480 and selumetinib on cell survival and signaling pathways in ALL xenografts. A–H, sensitivity of JAK-mutated (A–E) and JAK wild-type (F–I) xenografts to *in vitro* fixed ratios of single agents and the combination of AZD1480 and selumetinib. After 72 hours, drug exposure cell viability assessed by AlamarBlue assay. Each data point represents the mean ± SEM of 3 independent experiments. J, Log_{10} CIs from xenografts shown in A–I, represented as mean ± SE. K, mean CIs of JAK-mutated and JAK wild-type xenografts were compared using the Student *t* test. L and M, effects of AZD1480 and selumetinib alone and in combination on candidate signaling pathways in PALLSD (L) and PAMDRM (M). Cells were exposed to each drug (1 μmol/L) alone or in combination for up to 24 hours and cell extracts analyzed by immunoblotting.

of selumetinib in humans was a median of 8.3 hours (36), and increased with increasing dose, while sustained inhibition of pERK was observed in circulating lymphocytes from patients treated on a prolonged twice daily dosing regimen. The rapid plasma clearance of AZD1480 and selumetinib, along with our inability to coadminister the higher doses more frequently than once daily due to toxicity issues, are likely to have significantly contributed to our failure to translate their impressive *in vitro* synergy to the *in vivo* setting.

Inhibition of the MAPK pathway results in activation of the PI3K/AKT pathway in breast cancer cells (32, 33), and the combination of MEK and mTOR inhibitors exerted synergistic anticancer activity both *in vitro* and *in vivo* (33). However, given the difficulty we experienced in optimizing a tolerable combination schedule of AZD1480 and selumetinib in NOD/SCID mice, it was not possible to include an mTOR inhibitor in our *in vivo* combination studies. As CRLF2 is capable of activating the JAK/STAT, MAPK, and PI3K/AKT pathways (5–10), and given the current problems associated with the therapeutic use of small-molecule JAK inhibitors (37), CRLF2 may represent a more promising target for drug development in the treatment of JAK-mutated/CRLF2-rearranged ALL, although such inhibitors remain to be developed and tested in the preclinical setting.

Despite the disappointing outcome of our efficacy experiments testing the *in vivo* combination of AZD1480 and selumetinib, other JAK inhibitors may be useful for the treatment of JAK-mutated ALL. Although the clinical development of AZD1480 has recently been halted due to dose-limiting toxicities (35), our data clearly demonstrate that AZD1480 was able to inhibit its target *in vivo*, albeit briefly. Other JAK inhibitors such as ruxolitinib, TGT101348, and CYT387 have demonstrated clinical safety and efficacy in other malignancies (16, 17, 38), and ruxolitinib in

Published OnlineFirst December 10, 2014; DOI: 10.1158/1535-7163.MCT-14-0647

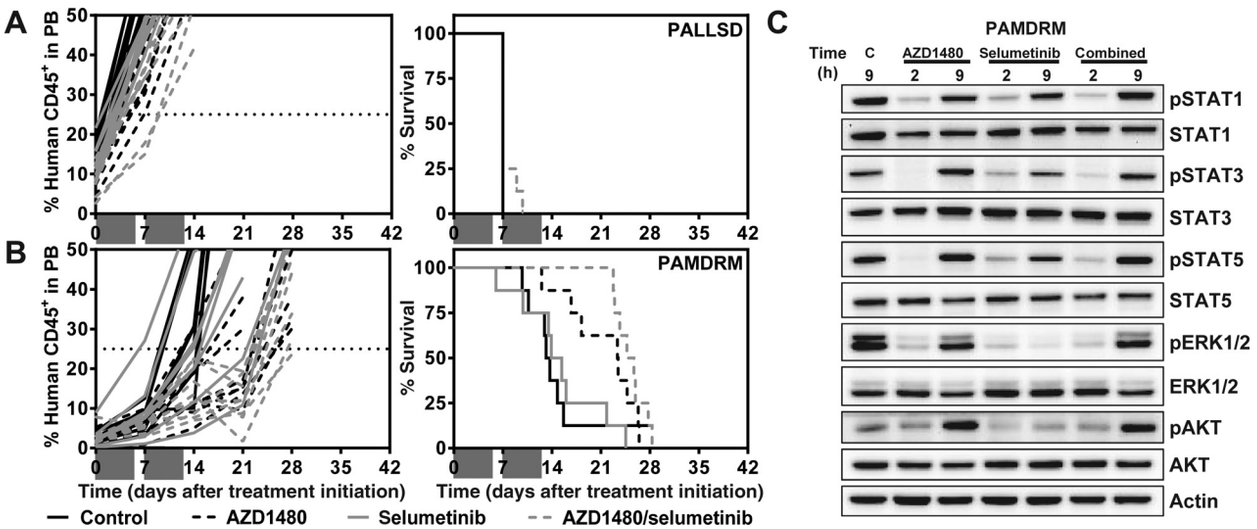

Figure 5.

In vivo efficacy of the combination of AZD1480 and selumetinib. Mice inoculated with PALLSD (A) or PAMDRM (B) were randomized to receive vehicle control or treatment with AZD1480 or selumetinib either as single agents or combination, as described in the Materials and Methods. Results are presented as the percentage of huCD45$^+$ cells in the PB over time (left) or mouse EFS (right). Gray shading indicates the treatment period. C, pharmacodynamic analysis of ALL engrafted mice treated with AZD1480/selumetinib. Mice highly engrafted with PAMDRM cells were treated with vehicle control (M), AZD1480 (30 mg/kg), selumetinib (25 mg/kg), or selumetinib (25 mg/kg) 3 hours before AZD1480 (30 mg/kg). Spleens were collected at 2 and 9 hours after AZD1480 treatment. Vehicle-treated spleens were collected at the 9-hour timepoint. Protein extracts were analyzed by immunoblotting. Each lane is representative of a single spleen.

particular was efficacious against preclinical models of pediatric JAK-mutated ALL (23, 39). Thus, alternative JAK inhibitors, when used under conditions that can achieve prolonged target inhibition, may yet be efficacious in the treatment of JAK-mutated ALL.

In summary, this study has detailed the development and molecular characterization of a panel of patient-derived xenografts from Kinase-like/JAK-mutated pediatric ALL. These xenografts exhibited dysregulated activation of multiple signaling pathways, consistent with the primary disease, indicating that they provide a highly relevant preclinical experimental model. Despite strong evidence of target inhibition, a small-molecule JAK1/2 inhibitor exhibited modest *in vitro* and *in vivo* antileukemic efficacy against these xenografts, leading to rational targeting of dual signaling nodes that resulted in profound *in vitro* drug synergy. Translation of these synergistic drug interactions to the *in vivo* setting, however, appeared to require sustained target inhibition that was not achievable using tolerable drug dosing and administration schedules in experimental mouse models.

Disclosure of Potential Conflicts of Interest

M.L. Loh is a consultant/advisory board member for Novartis. No potential conflicts of interest were disclosed by the other authors.

Disclaimer

Children's Cancer Institute Australia for Medical Research is affiliated with UNSW Australia and The Sydney Children's Hospitals Network.

Authors' Contributions

Conception and design: S. Suryani, H. Carol, C. Willman, P.J. Houghton, M.A. Smith, R.B. Lock

Development of methodology: S. Suryani, H. Carol, C.G. Mullighan, C. Willman, P.J. Houghton, R.B. Lock

Acquisition of data (provided animals, acquired and managed patients, provided facilities, etc.): S. Suryani, L.S. Bracken, K.C.S. Sia, H. Carol, K. Evans, P.A. Dietrich, C.G. Mullighan, C. Willman, M.L. Loh, S.P. Hunger

Analysis and interpretation of data (e.g., statistical analysis, biostatistics, computational analysis): S. Suryani, L.S. Bracken, R.C. Harvey, K.C.S. Sia, H. Carol, K.G. Roberts, R.T. Kurmasheva, C.A. Billups, C. Willman, P.J. Houghton, M.A. Smith, R.B. Lock

Writing, review, and/or revision of the manuscript: S. Suryani, L.S. Bracken, R.C. Harvey, K.C.S. Sia, C. Willman, S.P. Hunger, P.J. Houghton, M.A. Smith, R.B. Lock

Administrative, technical, or material support (i.e., reporting or organizing data, constructing databases): S. Suryani, L.S. Bracken, I.-M. Chen, K.G. Roberts, M.L. Loh

Study supervision: S. Suryani, P.J. Houghton, R.B. Lock

Acknowledgments

The authors thank AstraZeneca Pharmaceuticals for providing AZD1480 and selumetinib and the Children's Oncology Group for the provision of the P9906 primary patient samples.

Grant Support

This research was funded by grants from the National Cancer Institute including NOI-CM-42216 and NOI-CM-91001-03 (to P.J. Houghton), CA98543 (COG Chair's grant), CA98413 (COG Statistical Center) and CA114766 (COG Specimen Banking; to S.P. Hunger). S. Suryani is supported by Postdoctoral Fellowships from the Leukaemia Foundation of Australia and the Cure Cancer Australia Foundation, and an Early Career Fellowship from the Cancer Institute NSW. S.P. Hunger is the Ergen Family Chair in Pediatric Cancer. R.B. Lock is supported by a Fellowship from the National Health and Medical Research Council.

The costs of publication of this article were defrayed in part by the payment of page charges. This article must therefore be hereby marked *advertisement* in accordance with 18 U.S.C. Section 1734 solely to indicate this fact.

Received August 6, 2014; revised October 29, 2014; accepted November 13, 2014; published OnlineFirst December 10, 2014.

Published OnlineFirst December 10, 2014; DOI: 10.1158/1535-7163.MCT-14-0647

References

1. Pui CH, Mullighan CG, Evans WE, Relling MV. Pediatric acute lymphoblastic leukemia: where are we going and how do we get there? Blood 2012;120:1165–74.
2. Harvey RC, Mullighan CG, Wang X, Dobbin KK, Davidson GS, Bedrick EJ, et al. Identification of novel cluster groups in pediatric high-risk B-precursor acute lymphoblastic leukemia with gene expression profiling: correlation with genome-wide DNA copy number alterations, clinical characteristics, and outcome. Blood 2010;116:4874–84.
3. Harvey RC, Mullighan CG, Chen IM, Wharton W, Mikhail FM, Carroll AJ, et al. Rearrangement of CRLF2 is associated with mutation of JAK kinases, alteration of IKZF1, Hispanic/Latino ethnicity, and a poor outcome in pediatric B-progenitor acute lymphoblastic leukemia. Blood 2010;115:5312–21.
4. Mullighan CG, Zhang J, Harvey RC, Collins-Underwood JR, Schulman BA, Phillips LA, et al. JAK mutations in high-risk childhood acute lymphoblastic leukemia. Proc Natl Acad Sci U S A 2009;106:9414–8.
5. Mullighan CG, Collins-Underwood JR, Phillips LA, Loudin MG, Liu W, Zhang J, et al. Rearrangement of CRLF2 in B-progenitor- and Down syndrome-associated acute lymphoblastic leukemia. Nat Genet 2009;41:1243–6.
6. Roberts KG, Morin RD, Zhang J, Hirst M, Zhao Y, Su X, et al. Genetic alterations activating kinase and cytokine receptor signaling in high-risk acute lymphoblastic leukemia. Cancer Cell 2012;22:153–66.
7. Roll JD, Reuther GW. CRLF2 and JAK2 in B-progenitor acute lymphoblastic leukemia: a novel association in oncogenesis. Cancer Res 2010;70:7347–52.
8. Russell LJ, Capasso M, Vater I, Akasaka T, Bernard OA, Calasanz MJ, et al. Deregulated expression of cytokine receptor gene, CRLF2, is involved in lymphoid transformation in B-cell precursor acute lymphoblastic leukemia. Blood 2009;114:2688–98.
9. Tasian SK, Doral MY, Borowitz MJ, Wood BL, Chen IM, Harvey RC, et al. Aberrant STAT5 and PI3K/mTOR pathway signaling occurs in human CRLF2-rearranged B-precursor acute lymphoblastic leukemia. Blood 2012;120:833–42.
10. van Bodegom D, Zhong J, Kopp N, Dutta C, Kim MS, Bird L, et al. Differences in signaling through the B-cell leukemia oncoprotein CRLF2 in response to TSLP and through mutant JAK2. Blood 2012;120:2853–63.
11. Steelman LS, Pohnert SC, Shelton JG, Franklin RA, Bertrand FE, McCubrey JA. JAK/STAT, Raf/MEK/ERK, PI3K/Akt and BCR-ABL in cell cycle progression and leukemogenesis. Leukemia 2004;18:189–218.
12. Flex E, Petrangeli V, Stella L, Chiaretti S, Hornakova T, Knoops L, et al. Somatically acquired JAK1 mutations in adult acute lymphoblastic leukemia. J Exp Med 2008;205:751–8.
13. Zhang J, Mullighan CG, Harvey RC, Wu G, Chen X, Edmonson M, et al. Key pathways are frequently mutated in high-risk childhood acute lymphoblastic leukemia: a report from the Children's Oncology Group. Blood 2011;118:3080–7.
14. Chang F, Lee JT, Navolanic PM, Steelman LS, Shelton JG, Blalock WL, et al. Involvement of PI3K/Akt pathway in cell cycle progression, apoptosis, and neoplastic transformation: a target for cancer chemotherapy. Leukemia 2003;17:590–603.
15. Lim J, Taoka B, Otte RD, Spencer K, Dinsmore CJ, Altman MD, et al. Discovery of 1-amino-5H-pyrido[4,3-b]indol-4-carboxamide inhibitors of Janus kinase 2 (JAK2) for the treatment of myeloproliferative disorders. J Med Chem 2011;54:7334–49.
16. Pardanani A, Gotlib JR, Jamieson C, Cortes JE, Talpaz M, Stone RM, et al. Safety and efficacy of TG101348, a selective JAK2 inhibitor, in myelofibrosis. J Clin Oncol 2011;29:789–96.
17. Tyner JW, Bumm TG, Deininger J, Wood L, Aichberger KJ, Loriaux MM, et al. CYT387, a novel JAK2 inhibitor, induces hematologic responses and normalizes inflammatory cytokines in murine myeloproliferative neoplasms. Blood 2010;115:5232–40.
18. Barrio S, Gallardo M, Arenas A, Ayala R, Rapado I, Rueda D, et al. Inhibition of related JAK/STAT pathways with molecular targeted drugs shows strong synergy with ruxolitinib in chronic myeloproliferative neoplasm. Br J Haematol 2013;161:667–76.
19. Chase A, Bryant C, Score J, Haferlach C, Grossmann V, Schwaab J, et al. Ruxolitinib as potential targeted therapy for patients with JAK2 rearrangements. Haematologica 2013;98:404–8.
20. Hedvat M, Huszar D, Herrmann A, Gozgit JM, Schroeder A, Sheehy A, et al. The JAK2 inhibitor AZD1480 potently blocks Stat3 signaling and oncogenesis in solid tumors. Cancer Cell 2009;16:487–97.
21. Ioannidis S, Lamb ML, Wang T, Almeida L, Block MH, Davies AM, et al. Discovery of 5-chloro-N2-[(1S)-1-(5-fluoropyrimidin-2-yl)ethyl]-N4-(5-methyl-1H-pyrazol-3-yl)p yrimidine-2,4-diamine (AZD1480) as a novel inhibitor of the Jak/Stat pathway. J Med Chem 2011;54:262–76.
22. Schultz KR, Bowman WP, Aledo A, Slayton WB, Sather H, Devidas M, et al. Improved early event-free survival with imatinib in Philadelphia chromosome-positive acute lymphoblastic leukemia: a children's oncology group study. J Clin Oncol 2009;27:5175–81.
23. Maude SL, Tasian SK, Vincent T, Hall JW, Sheen C, Roberts KG, et al. Targeting JAK1/2 and mTOR in murine xenograft models of Ph-like acute lymphoblastic leukemia. Blood 2012;120:3510–8.
24. Dry JR, Pavey S, Pratilas CA, Harbron C, Runswick S, Hodgson D, et al. Transcriptional pathway signatures predict MEK addiction and response to selumetinib (AZD6244). Cancer Res 2010;70:2264–73.
25. Houghton PJ, Morton CL, Tucker C, Payne D, Favours E, Cole C, et al. The pediatric preclinical testing program: description of models and early testing results. Pediatr Blood Cancer 2007;49:928–40.
26. Liem NL, Papa RA, Milross CG, Schmid MA, Tajbakhsh M, Choi S, et al. Characterization of childhood acute lymphoblastic leukemia xenograft models for the preclinical evaluation of new therapies. Blood 2004;103:3905–14.
27. Lock RB, Liem N, Farnsworth ML, Milross CG, Xue C, Tajbakhsh M, et al. The nonobese diabetic/severe combined immunodeficient (NOD/SCID) mouse model of childhood acute lymphoblastic leukemia reveals intrinsic differences in biologic characteristics at diagnosis and relapse. Blood 2002;99:4100–8.
28. Houghton PJ, Morton CL, Gorlick R, Lock RB, Carol H, Reynolds CP, et al. Stage 2 combination testing of rapamycin with cytotoxic agents by the Pediatric Preclinical Testing Program. Mol Cancer Ther 2010;9:101–12.
29. Rose WC, Wild R. Therapeutic synergy of oral taxane BMS-275183 and cetuximab versus human tumor xenografts. Clin Cancer Res 2004;10:7413–7.
30. Bachmann PS, Gorman R, Papa RA, Bardell JE, Ford J, Kees UR, et al. Divergent mechanisms of glucocorticoid resistance in experimental models of pediatric acute lymphoblastic leukemia. Cancer Res 2007;67:4482–90.
31. Mullighan CG, Su X, Zhang J, Radtke I, Phillips LA, Miller CB, et al. Deletion of IKZF1 and prognosis in acute lymphoblastic leukemia. N Engl J Med 2009;360:470–80.
32. Duncan JS, Whittle MC, Nakamura K, Abell AN, Midland AA, Zawistowski JS, et al. Dynamic reprogramming of the kinome in response to targeted MEK inhibition in triple-negative breast cancer. Cell 2012;149:307–21.
33. Hoeflich KP, O'Brien C, Boyd Z, Cavet G, Guerrero S, Jung K, et al. In vivo antitumor activity of MEK and phosphatidylinositol 3-kinase inhibitors in basal-like breast cancer models. Clin Cancer Res 2009;15:4649–64.
34. Koppikar P, Bhagwat N, Kilpivaara O, Manshouri T, Adli M, Hricik T, et al. Heterodimeric JAK-STAT activation as a mechanism of persistence to JAK2 inhibitor therapy. Nature 2012;489:155–9.
35. Plimack ER, Lorusso PM, McCoon P, Tang W, Krebs AD, Curt G, et al. AZD1480: a phase I study of a novel JAK2 inhibitor in solid tumors. Oncologist 2013;18:819–20.
36. Adjei AA, Cohen RB, Franklin W, Morris C, Wilson D, Molina JR, et al. Phase I pharmacokinetic and pharmacodynamic study of the oral, small-molecule mitogen-activated protein kinase kinase 1/2 inhibitor AZD6244 (ARRY-142886) in patients with advanced cancers. J Clin Oncol 2008;26:2139–46.
37. Trelinski J, Robak T. JAK inhibitors: pharmacology and clinical activity in chronic myeloprolipherative neoplasms. Curr Med Chem 2013;20:1147–61.
38. Pardanani A, Laborde RR, Lasho TL, Finke C, Begna K, Al-Kali A, et al. Safety and efficacy of CYT387, a JAK1 and JAK2 inhibitor, in myelofibrosis. Leukemia 2013;27:1322–7.
39. Roberts KG, Li Y, Payne-Turner D, Harvey RC, Yang YL, Pei D, et al. Targetable kinase-activating lesions in Ph-like acute lymphoblastic leukemia. N Engl J Med 2014;371:1005–15.

Published OnlineFirst December 10, 2014; DOI: 10.1158/1535-7163.MCT-14-0647

Molecular Cancer Therapeutics

Evaluation of the *In Vitro* and *In Vivo* Efficacy of the JAK Inhibitor AZD1480 against JAK-Mutated Acute Lymphoblastic Leukemia

Santi Suryani, Lauryn S. Bracken, Richard C. Harvey, et al.

Mol Cancer Ther 2015;14:364-374. Published OnlineFirst December 10, 2014.